(This is a sample cover image for this issue. The actual cover is not yet available at this time.)

Mechanics Research Communications 44 (2012) 47–50

Contents lists available at SciVerse ScienceDirect

Mechanics Research Communications

journal homepage: www.elsevier.com/locate/mechrescom

Reynolds number dependence of near field vortex motion downstream from an asymmetrical nozzle

A. Van Hirtum*, X. Grandchamp, J. Cisonni

GIPSA-lab, UMR CNRS 5216, Grenoble University, France

ARTICLE INFO

Article history:
Received 2 February 2012
Available online xxx

Keywords:
Moderate Reynolds number flow
Plane jet
Smoke visualisation
Vortex motion

ABSTRACT

Smoke visualisation is used to quantify the influence of low to moderate Reynolds number (<1100) on near field vortex motion downstream from an asymmetrical nozzle. The influence of Reynolds number is found to be predominant for low Reynolds numbers (<500). The relationship between Reynolds number and vortex shedding is assessed.

1. Introduction

There is significant interest in low and moderate speed jets within the context of naturally occurring jets such as is the case during human speech sound production (Fabre et al., 2012). Indeed, the Reynolds numbers associated with human speech sound production are $Re_b < 10^4$ so that low and moderate speed jet formation occurs at a constriction along the vocal tract (e.g. at the glottis during voiced sound production or downstream from the teeth during fricative sibilant sound production). In addition, it is well accepted to make severe simplifications of the geometry of interest, so that the vocal tracts geometry is commonly represented as a rigid circular tube or a rectangular channel (Fabre et al., 2012; Cisonni et al., 2008; Van Hirtum et al., 2011). Consequently, in case a rectangular channel is used (Cisonni et al., 2008; Van Hirtum et al., 2011) a plane jet is formed. Despite numerous experimental and numerical studies of plane jets, most research focus on high Reynolds number flow ($Re_b > 10^4$) and well designed nozzles due to their importance for technological applications. As a consequence, several authors report the lack of data in relation to jets at low or moderate Reynolds numbers in general (Grinstein, 2001; Schneider and Goldstein, 1994; Launder and Rodi, 1983; Gutmark and Ho, 1983) or in relation to biofluid mechanics such as human speech production (Howe and McGowan, 2005; Bodony, 2005). In the current study, smoke visualisation is used to quantify the influence of low to moderate Reynolds number on near field vortex motion downstream from an asymmetrical nozzle.

2. Experimental approach

The asymmetrical nozzle consists of a sharp obstacle inserted in a rectangular channel as depicted in Fig. 1(a). The obstacle consists of a trapezoidal wedge shaped as an upper incisor (Pound, 1976; Grandchamp, 2009). The nozzle is attached to a settling chamber to which smoke can be injected. Two-dimensional illumination is applied with a two-dimensional laser light beam (class IIIb). The illuminated smoke pattern is recorded at 300 fps (Casio, EXILIM Pro EX-F1) which ensures a good freezing of the flow development. The digitised two-dimensional images are 512×384 data matrices. Spatial calibration of the images is performed. Experimental conditions are summarised in Table 1.

Vortex motion is tracked in the two-dimensional flow images by locating a rectangle envelope for each individual vortex as illustrated in Fig. 1(b). Detection of spatial features (centre position, height and width) of rectangles enveloping counterclockwise (cc) and clockwise (c) vortices in consecutive images allows to quantify vortex convection velocity U_{conv} and vortex shedding frequency f_v. For each assessed Reynolds number vortex feature detection is applied on 4000 consecutive images, which is large compared to typical numbers reported in literature (300 (Smith and Dutton, 1999) up to 2000 (Iio et al., 2008)). Three counterclockwise (cc) and three clockwise (c) vortices are characterised in each image.

3. Results

3.1. Spatial occurrence: mean centre position

Normalised mean centre positions $(\bar{x}/h, \bar{y}/h)$ of the enveloping rectangles are located in the range $3 < \bar{x}/h < 13$ and $0.5 < |\bar{y}/h| <$

* Corresponding author.

0093-6413/$ – see front matter © 2012 Elsevier Ltd. All rights reserved.
http://dx.doi.org/10.1016/j.mechrescom.2012.05.003

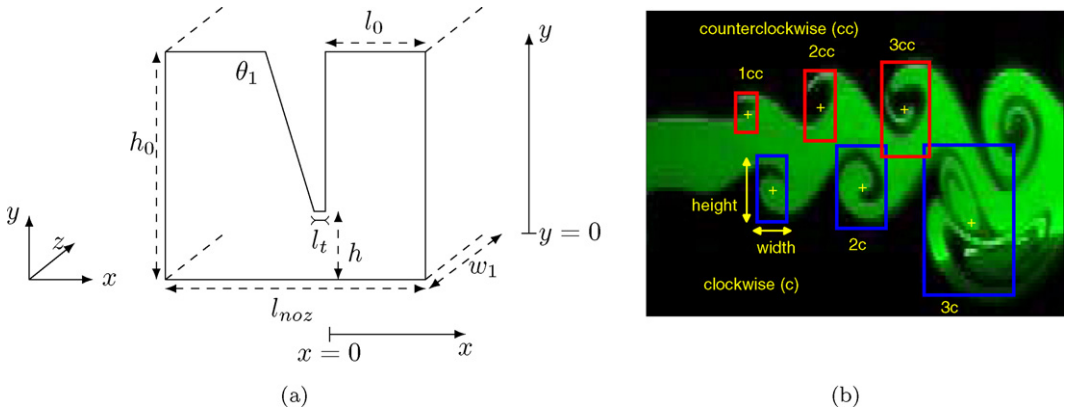

Fig. 1. (a) Schematic representation of the asymmetrical nozzle: $h = 7.5$ mm, $l_0 = 11$ mm, $h_0 = 25$ mm, $w_1 = 105$ mm, $l_t = 1.2$ mm, $\theta_1 = 107^\circ$ and $l_{noz} = 360$ mm. The x and y axis correspond to the main flow direction and the transverse direction perpendicular to the flat wall, respectively. The origin of the transverse y axis is chosen so that the aperture spans $-h/2 \leq y \leq h/2$. (b) Illustration of spatial vortex features derived from an enveloping rectangle on each individual flow visualisation image: centre position (+), height and width.

Table 1
Overview of experimental conditions: volume flow rate Q, bulk Reynolds numbers $Re_b = Q/\nu w_1$ and bulk velocities $U_0 = Q/hw_1$ at the minimum constriction with air kinematic viscosity $\nu = 1.5 \times 10^{-5}$ m^2/s.

Q [l/min]	12	14	17	25	38	67	102
Re_b	127	148	170	265	402	709	1079
U_0 [m/s]	0.25	0.30	0.36	0.53	0.80	1.42	2.16

1.1 (Fig. 2(a)). Mean locations are subject to a standard deviation due to vortex convection ($\Delta\bar{x}/h < 0.9$ and $\Delta\bar{y}/h < 0.15$), which is within the range reported in literature (Smith and Dutton, 1999; Morse and Liburdy, 2009). The spatial life-span of the identified vortices shortens as Re_b increases. This is in agreement with findings observed for plane jets at higher Reynolds numbers $Re_b > 5 \times 10^3$ (Deo et al., 2008) for which an increase in Re_b enforces flow entrainment so that the potential core extent decreases. Nevertheless, in contrast to instantaneous observations made on symmetrical plane nozzles, an important spatial asymmetry is observed for the mean centre locations of counterclockwise and clockwise vortices as shown in Fig. 2(b) for $\bar{x}_{cc}/\bar{x}_c$ and in Fig. 2(c) for $|\bar{y}_{cc}/\bar{y}_c|$. The asymmetry increases as the Reynolds number decreases for both the longitudinal and the transverse coordinate and becomes predominant for $Re_b < 500$.

3.2. Spatial vortex growth: width-to-height ratio

The width-to-height ratio R of each rectangle informs on the deformation from a squared vortex envelop ($R = 1$): streamwise stretching ($1 < R$) or transverse stretching ($0 < R < 1$). Mean ratios $\bar{R}$ as function of Re_b are illustrated in Fig. 3. In general, it is observed that transverse stretching reduces with Reynolds number. The growth rate of R in the streamwise direction x/h is estimated from linear regression of $R(x/h)$ on all data images of each Reynolds number. The error on regression parameters is less than 3% due to the large number of data images. In Fig. 3(b) streamwise growth rates $dR/d(x/h)$ are shown as function of Re_b. The growth rate decreases as the Reynolds number Re_b increases and is approximated as $dR/d(x/h)(Re_b) = 0.96 \times Re_b^{-0.41}$. The functional relationship $dR/d(x/h)(Re_b)$ is comparable with the relationship to describe wavelength (λ) decrease of the shear-layer instability for transition of low Reynolds incompressible flow around a wing, $\lambda \propto Re^{-0.44}$ (Hoarau et al., 2003).

3.3. Time evolution

Estimated vortex shedding frequencies f_v (Fig. 4(a)) increase linearly with Re_b and the relationship can be approximated as $f_v(Re_b) \approx 0.14 \times Re_b - 8$. Frequencies derived for counterclockwise and clockwise vortices match.

The estimated streamwise vortex convection velocities U_{conv} (Fig. 4(b)) approximate bulk velocities for low Reynolds numbers $Re_b < 500$, $U_{conv} \approx U_0$. Nevertheless, in general $U_{conv} < U_0$ holds and U_{conv} increases linearly with Reynolds number for $Re_b < 800$. Values for $Re_b = 1079$ approximate values for $Re_b = 709$. The difference between U_{conv} and U_0 expressed as U_{conv}/U_0 for $Re_b < 800$ remains <20% for clockwise vortices and <30% for counterclockwise vortices. Retrieved values are larger than values reported for plane jet studies with $Re_b > 2000$ (Sato, 1960; Ho and Huerre, 1984; Hsiao et al., 2010) and approximate values retrieved for plane jets at $Re_b > 10000$ (Gutmark and Ho, 1983).

The linear approximation, $f_v(Re_b) \approx \alpha Re_b + \beta$ with regression parameters ($\alpha = 0.14$, $\beta = -8$), is used to derive the Strouhal number $St = f_v h/U_0$ associated with vortex shedding as function of Reynolds number Re_b:

$$St(Re_b) \approx \left[\alpha + \frac{\beta}{Re_b}\right] \frac{h^2}{\nu}.$$

Strouhal numbers $St(Re_b)$, shown in Fig. 5(a), vary in the range $0.3 < St(Re_b) < 0.55$ and increase with Re_b. Consequently, as the Reynolds number increases vortex shedding becomes more important compared to convection confirming the narrowed spatial vortex distribution as Re_b increases.

The estimation of f_v from the vortex shedding period does not distinguish between shear-layer mode or preferred mode. Nevertheless, since the estimation is obtained on vortices in the near field region, it is motivated to assume that obtained f_v values are associated with the shear-layer mode as already suggested from the spatial growth rate R. This might partly explain the high values in the current study compared to St values, $0.1 < St < 0.3$, typically associated with two-dimensional jets for both the anti-symmetric and symmetric mode and this despite the fact that assessed Reynolds numbers $100 < Re_b < 1100$ are smaller than studied in Ho and Huerre (1984), Hsiao and Huang (1990), Deo et al. (2008) and Hsiao et al. (2010). Therefore, the observed discrepancy with reported St values is the result of the difference in flow

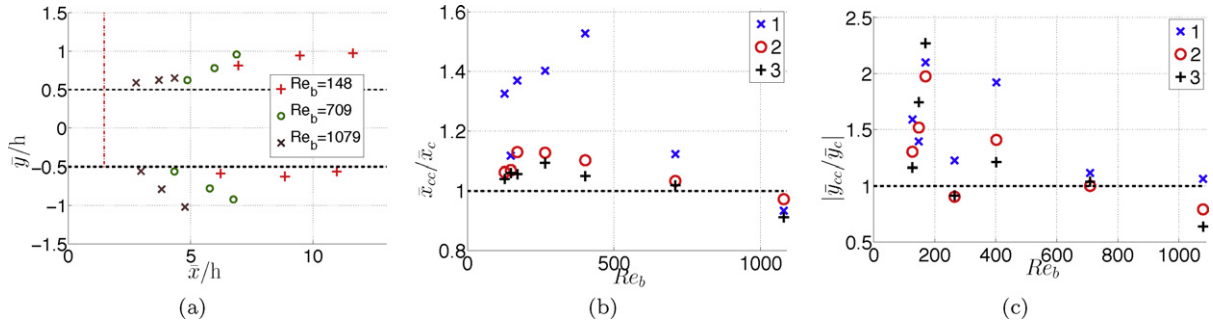

Fig. 2. (a) Illustration of normalised mean centre locations $(\bar{x}/h, \bar{y}/h)$ for $Re_b \in \{148, 709, 1079\}$. The vertical dashed line indicates the nozzle outlet and the horizontal dashed lines mark the transverse aperture of the obstacle tip $-0.5 < y/h < 0.5$. (b and c) Spatial asymmetry between counterclockwise (cc) and clockwise (c) vortices expressed as $\bar{x}_{cc}/\bar{x}_c$ (b) and $|\bar{y}_{cc}/\bar{y}_c|$ (c) as function of Re_b. The dashed line denotes a symmetrical condition corresponding to ratios equal to 1.

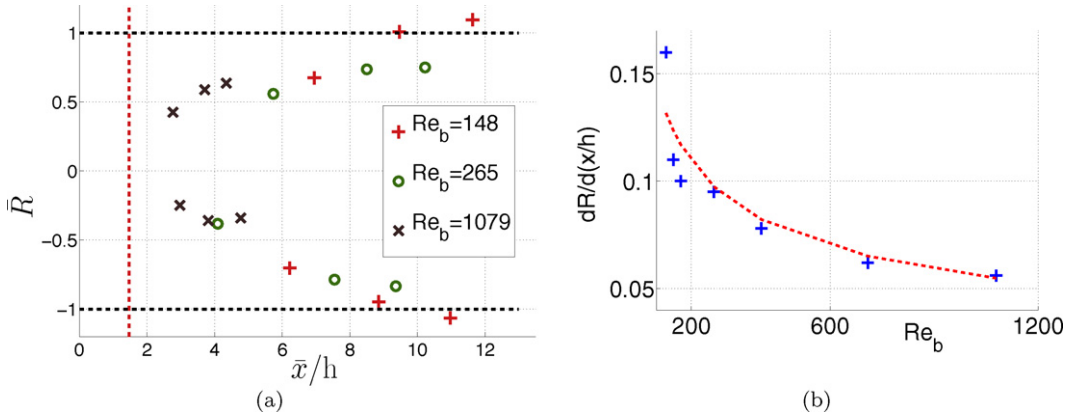

Fig. 3. (a) Illustration of mean width-to-height ratios $\bar{R}$ as function of mean streamwise centre position $\bar{x}/h$ for clockwise ($-\bar{R} < 0$) and counterclockwise ($\bar{R} > 0$) vortices for $Re_b \in \{148, 709, 1079\}$. The vertical dashed line at $x/h = 1.47$ indicates the nozzle outlet. The vortex stretching is streamwise for $|R| > 1$ and transverse for $|R| < 1$. The transition $|R| = 1$ is indicated by a horizontal dashed line. (b) The growth speed of the width-to-height ratio in the streamwise direction as a function of Reynolds number $dR/d(x/h)(Re_b)$ and the functional approximation $\approx 0.96 \times Re_b^{-0.41}$ (dashed curve).

structure due to the asymmetry of the nozzle compared to plane jet studies (Ho and Huerre, 1984; Hsiao and Huang, 1990; Deo et al., 2008; Hsiao et al., 2010). In particular an asymmetrical initial velocity profile and associated momentum thickness is created at the obstacle, $x/h = 0$, due to an asymmetrical flow acceleration upstream from the constriction in contrary to symmetrical initial flow profiles (uniform, 'top-hat' or power-law) assumed or measured in plane jet studies (Sato, 1960; Ho and Huerre, 1984; Hsiao et al., 2010). The velocity profile needs to be studied in more detail since it alters the vortex dynamics compared to the mentioned studies resulting in: increased vortex shedding frequency f_v, increased convection velocity U_{conv}, increased St and asymmetrical spatial vortex behaviour. The non dimensional ratio $(U_0/l_0)/f_v$ (Fig. 5(b)) decreases quickly to $(U_0/l_0)/f_v \approx 1.5$ for low Reynolds numbers ($Re_b < 500$), for which the Reynolds number dependence is most evident. Therefore, the ratio $(U_0/l_0)/f_v$ might be a measure for Reynold number sensitivity as it is related to convection (U_0) as well as vortex shedding (f_v). It is seen that the value 1.5 approximates the ratio of the nozzle length downstream from the obstacle to the aperture $l_0/h = 1.47 \approx 1.5$, which motivates

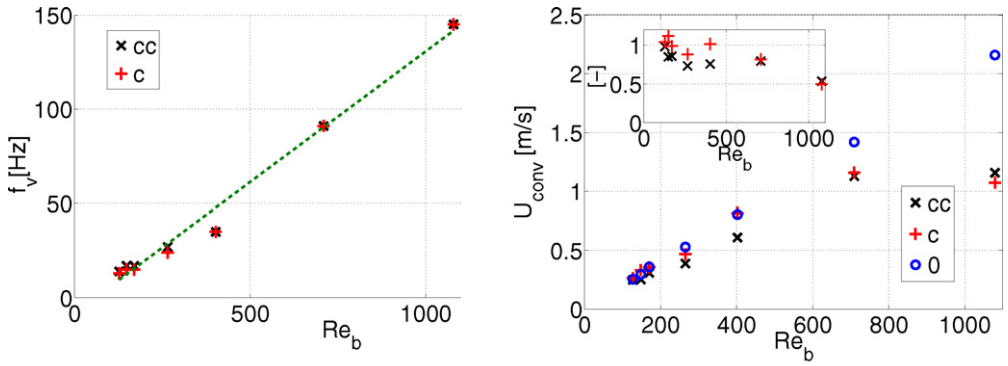

Fig. 4. Estimation of (a) vortex shedding frequency $f_v(Re_b)$ [Hz] and approximation as $f_v(Re_b) \approx 0.14 \times Re_b - 8$. (b) Streamwise vortex convection velocity $U_{conv}(Re_b)$ [m/s] for counterclockwise (×) and clockwise (+) vortices. As a reference also the bulk velocity at the minimum aperture $U_0(Re_b)$ (o) [m/s] is indicated. The ratios $U_{conv}/U_0(Re_b)$ [-] are illustrated as well (inner frame).

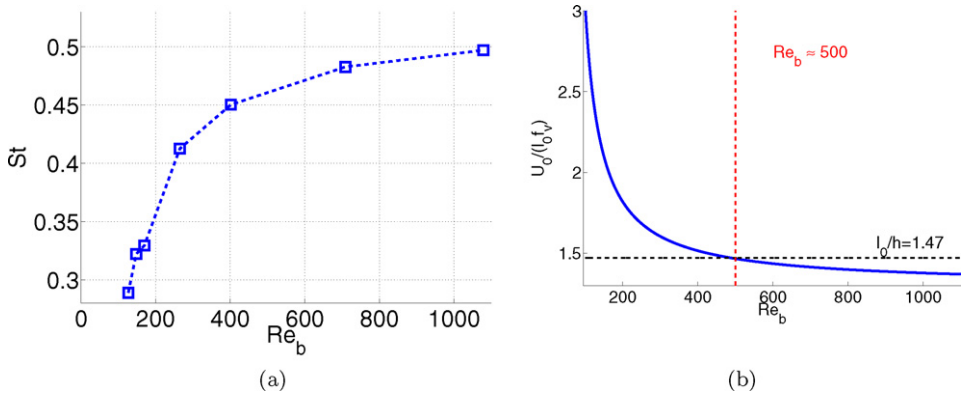

Fig. 5. (a) Strouhal numbers $St(Re_b)$ resulting from f_v-values for counterclockwise (cc) and clockwise (c) vortices (□) as well as from the linear approximation $f_v(Re_b, h) \approx 0.14 \times Re_b - 8$ (dashed). (b) Non dimensional ratio $(U_0/l_0)/f_v$ as function of Re_b.

further study of the influence of the geometrical parameters h and l_0 on the flow development.

4. Conclusion

With respect to the influence of Reynolds number, $100 < Re_b < 1100$, on vortex motion downstream from an asymmetrical nozzle, it is seen that as the Reynolds number increases: the asymmetry between counterclockwise and clockwise vortices expressed by the mean centre locations of the enveloping rectangle decreases, transverse vortex stretching reduces, the vortex shedding frequency increases linearly and the associated Strouhal number increases. Derived functional relationships for vortex frequency and Strouhal number need to be validated as well as the suggestion that vortex shedding is associated with the shear-layer mode of Kelvin–Helmholtz vortices. Finally, the influence of Reynolds number is found to be predominant for low Reynolds numbers $Re_b < 500$. Velocity measurements of initial conditions and of the flow field need to be assessed in order to confirm and elaborate current results and in order to quantify important kinematic flow features such as vorticity moments.

References

Bodony, D., 2005. The Prediction and Understanding of Jet Noise. Center for Turbulence Research Annual Research Briefs, 367–377.
Cisonni, J., Van Hirtum, A., Pelorson, X., Willems, J., 2008. Theoretical simulation and experimental validation of inverse quasi one-dimensional steady and unsteady glottal flow models. The Journal of the Acoustical Society of America 124, 535–545.
Deo, R.C., Mi, J., Nathan, G.J., 2008. The influence of Reynolds number on a plane jet. Physics of Fluids 20, 1–16.
Fabre, B., Gilbert, J., Hirschberg, A., Pelorson, X., 2012. Aeroacoustics of musical instruments. Annual Review of Fluid Mechanics 44, 1–25.
Grandchamp, X., 2009. Modélisation physique des écoulements turbulents appliquées aux voies aériennes supérieures chez l'humain. PhD Thesis. Grenoble University.
Grinstein, F.F., 2001. Vortex dynamics and entrainment in rectangular free jets. Journal of Fluid Mechanics 437, 69–101.
Gutmark, E., Ho, C.M., 1983. Preferred modes and the spreading rates of jets. Physics of Fluids 26, 2932–2938.
Ho, C., Huerre, P., 1984. Perturbed free shear layers. Annual Review of Fluid Mechanics 16, 365–424.
Hoarau, Y., Braza, M., Ventikos, Y., Fahani, D., Tzabiras, G., 2003. Organized modes and the three-dimensional transition to turbulence in the incompressible flow around a NACA0012 wing. Journal of Fluid Mechanics 496, 63–72.
Howe, M., McGowan, R., 2005. Aeroacoustics of [s]. Proceedings of the Royal Society of London Series A 461, 1005–1028.
Hsiao, F., Huang, J., 1990. On the evolution of instabilities in the near field of a plane jet. Physics of Fluids 2, 400–412.
Hsiao, F., Lim, Y., Huang, J., 2010. On the near-field flow structure and mode behaviors for the right-angle and sharp-edged orifice plane jet. Experimental Thermal and Fluid Science 34, 1282–1289.
Iio, S., Takahashi, K., Haneda, Y., Ikeda, T., 2008. Flow visualisation of vortex structure in a pulsed rectangular jet. Journal of Visualization 11, 125–132.
Launder, B.E., Rodi, W., 1983. The turbulent wall jet-measurements and modeling. Annual Review of Fluid Mechanics 15, 429–459.
Morse, D.R., Liburdy, J.A., 2009. Vortex dynamics and shedding of a low aspect ratio, flat wing at low Reynolds numbers and high angles of attack. Journal of Fluids Engineering 131, 1–12.
Pound, E., 1976. Controlling anomalies of vertical dimension and speech. Journal of Prosthetic Dentistry 36, 124–135.
Sato, H., 1960. The stability and transition of a two-dimensional jet. Journal of Fluid Mechanics 7, 53–80.
Schneider, M.E., Goldstein, R.J., 1994. Laser Doppler measurement of turbulence parameters in a two-dimensional plane wall jet. Physics of Fluids 6, 3116–3129.
Smith, K.M., Dutton, J.C., 1999. A procedure for turbulent structure convection velocity measurements using time-correlated images. Experiments in Fluids 27, 244–250.
Van Hirtum, A., Pelorson, X., Estienne, O., Bailliet, H., 2011. Experimental validation of flow models for a rigid vocal tract replica. The Journal of the Acoustical Society of America 130, 2128–2138.